Tribology of hard particles lubricating soft surfaces

Physical Review Materials

Rudge, Raisa E.D.; Theunissen, Karlijn; Stokes, Jason R.; Scholten, Elke; Dijksman, Joshua A.

https://doi.org/10.1103/PhysRevMaterials.5.055604

Tribology of hard particles lubricating soft surfaces

Raisa E. D. Rudge,[1,2,*] Karlijn Theunissen,[1] Jason R. Stokes,[3] Elke Scholten,[2] and Joshua A. Dijksman[1]

[1]*Physical Chemistry and Soft Matter, Wageningen University, 6708 WE, The Netherlands*

[2]*Physics and Physical Chemistry of Foods, Wageningen University, 6708 WG, The Netherlands*

[3]*School of Chemical Engineering, The University of Queensland, 4072 Brisbane, Australia*

(Received 14 December 2020; accepted 6 April 2021; published xxxxxxxxxx)

Soft materials often have interesting and unexpected frictional behavior owing to their deformable nature. We use soft polydimethylsiloxane (PDMS) surfaces lubricated by hard glass spheres to study how this deformability influences particle-based lubrication. For particles between 100 and 2000 μm in size, we observe a nontrivial rate dependence and three frictional regimes: (I) a rolling friction regime where the rolling particles keep the surfaces apart sufficiently to give low friction coefficients—this is mainly found for large particles and smooth surfaces; (II) a sliding friction regime with high friction coefficients where the surfaces are partially in contact, which is found for small particles, rough surfaces, and high normal forces; (III) a PDMS-PDMS contact regime where the particles are fully inserted into surfaces and the surfaces are in contact. We interpret the friction dynamics in terms of the Hertzian contact deformation effects in the indentation of the PDMS surfaces.

DOI: 10.1103/PhysRevMaterials.00.005600

I. INTRODUCTION

To reduce the friction between two sliding surfaces under given normal load, typically, one uses either a lubricating fluid film or solid ball bearings. Lubrication films have been studied for a long time; Reynolds [1] already proposed an equation based on hydrodynamic pressure for such films [2]. Ball bearing lubrication has also been a subject of much interest throughout the past century [3–7]. The ability of ball bearings to reduce friction, wear, and subsequent energy losses has made these rolling elements of great importance to society with applications from computer components [8] to aerospace machinery [9,10].

In many fluid lubricated tribological systems, complex mechanics and nontrivial lubricant properties dictate the frictional behavior, and complexity is often the rule rather than the exception. The use of particles or *third bodies* between sliding surfaces should simply lead to a smaller real contact area between the sliding surfaces and subsequently decreases the friction coefficient. Many third-body lubrication studies consider only hard surfaces with hard particles for which surface deformation is negligible [11–13]. In soft material friction, however, the deformability of the involved materials becomes an additional important factor when third bodies are introduced, which should add interesting physics and potentially make it easier to clarify the physics of third-body friction, as pressures and time scales in tribological dynamics are reduced.

Many soft surfaces have been studied for their tribological behavior recently, including rubbers [14–16], hydrogels [17–19], and elastomers [20–22]. Such soft materials are found in a variety of applications, such as biomimetics, soft robotics cosmetics, and food materials. Most particle tribology studies involving soft materials use particles suspended in fluids instead of dry particles. For soft (hydrogel) particles in suspension, it was found that particle properties such as hardness, size, and volume fraction cause significant changes in the frictional behavior [23,24]. Using hard particles suspended in aqueous media, it was found that continuous phase viscosity, volume fraction, and particle-matrix entrainment are important parameters influencing the friction coefficient [25]. In general, more particles and less fluids leads to lower friction coefficients. In addition, under thin film (boundary) conditions, deformation of the substrate promotes entrainment of spherical particles, which have the ability to roll. Entrainment in the thin film regime is also found to depend on fluid-particle-substrate interaction.

Due to the complex interplay of the effect of suspended particles, fluid, and substrate, most studies, however, shed little light on how the particle phase influences the tribological behavior of the system in the absence of fluids. In this paper, we aim to uncover the particle contribution to friction, particularly the contributions of rolling and/or sliding mechanisms behind dry particle lubrication. To isolate particle-substrate interactions from fluid hydrodynamics and focus specifically on the effect of the lubricating particles on the frictional behavior of soft surfaces, we use dry hard glass particles and soft polydimethylsiloxane (PDMS) surfaces. Using this hard-soft tribosystem, we also consider the changes in the contact area associated with hard particles contacting soft substrates. Soft surface deformation is expected to cause (partial) particle penetration into the surfaces, which leads to increased contact area between the particles and the surfaces but also between surfaces for a large degree of deformation. These changes in contact dynamics could limit particle rolling ability. We test this hypothesis by systematically varying the surface roughness (smooth and rough) of the PDMS substrate,

*raisa.rudge@wur.nl

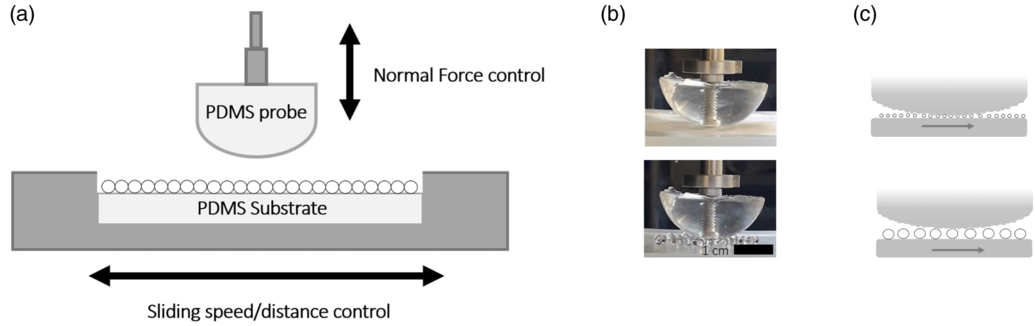

FIG. 1. (a) Schematic image of the measuring segment of the Bruker UMT Tribolab tribometer. (b) Image of the 2000 and 100 μm particles between polydimethylsiloxane (PDMS) surfaces together with a schematic representation of the particles between the surfaces.

the measuring speed (4–100 mm/s), particle size (100–2000 μm), particle number (10–100% surface coverage), and the ratio at which the surfaces slide alongside one another. Using such a systematic approach allows us to study how particles influence the frictional behavior in the absence of fluids. We present our results in terms of probe roughness, normal force, and number of spherical particles covering the surfaces.

II. FRICTION TESTS

In this paper, we used a Bruker UMT Tribolab tribometer [Fig. 1(a)] to measure the friction coefficient between a rough or smooth hemispherical probe ($R = 2$ cm) and flat substrate ($5.9 \times 4.4 \times 0.4$ cm), all made of PDMS (Sylgard 184 elastomer kit, 1:10 base:catalyst ratio). The rough probe (asperity size $\approx$ 100–400 μm) was obtained using a stainless steel mold (Eppicotispai Kitchenware). The tribological setup used consisted of a reciprocating substrate and a stationary probe. The oscillatory sliding distance was fixed at 10 mm, and we measured at maximum velocities from 4 to 100 mm/s at a fixed load of 0.5 N. As a lubricant, we introduced glass spheres in sizes of $\leqslant$106 μm (140-finer U.S. sieve), 212–300 μm, 425–600 μm (Sigma Aldrich), and $\sim$2000 μm (manufacturer unknown) to completely cover the substrate surface. The number of particles needed by weight was determined using the area of the substrate and the diameter of the particles together with the density of the particles. These spherical particles are referred to as 100, 300, 600, and 2000, respectively, throughout this paper. We show the smooth PDMS probe combined with the smallest and largest particles in Fig. 1(b). It should be noted that the presence of the metal screw inside the PDMS probe may decrease the deformability of the material.

To evaluate the effect of the relative speeds of sliding surfaces, we also used a PCS Instruments Mini Traction Machine (MTM) tribometer with a PDMS probe and substrate. The probe and the substrate on the MTM were driven by separate motors, allowing for variations between the speed ratio of the two. This ratio is known as the slide-to-roll ratio (SRR). The SRR is defined as SRR $= v_{\text{disk}} - v_{\text{ball}}/v_{\text{mean}}$ and $(v_{\text{mean}} = v_{\text{disk}} + v_{\text{ball}})/2$ [26–28]. An SRR $= 0$ corresponds to so-called "pure rolling," the the case where the ball and the disk rotate at the same speed in the same direction. An SRR $= 2$ refers to the ball rotating while the disk is stationary and vice versa. This is called "pure sliding." This pure sliding movement is most like the measurements performed with the Bruker UMT tribometer, where the substrates oscillate while the probe remains stationary.

III. RESULTS

Dry PDMS surfaces in direct contact can give friction coefficients as high as $\mu = 3$ due to the self-adhesive nature of PDMS [20,29]. To modulate the friction coefficient, we used spherical glass particles as our dry, solid lubricants. These particles were placed on the flat substrate to fully cover the surface (referred to as 100%). The particle sizes we used were 2000, 600, 300, and 100 μm. As shown in Fig. 2(a), these particles are able to generate a 100-fold decrease in friction coefficient with respect to bare PDMS-PDMS contacts to values as low as 0.02.

A. Particle size and sliding speed dependence

We find that the friction coefficient decreases with increasing particle size. For the largest particles, the friction coefficient ranges from 0.02 to 0.08 over the entire range of speeds, for the small particles, from 0.12 to 0.22 [Fig. 2(a)]. In the case of smaller particles, a larger number of glass particles is required to obtain the same surface coverage. This gives a larger number of separate surface-particle contacts, which we expect to contribute to a higher friction coefficient of the entire system. The number of contacts scales with the glass particle diameter R_g^2, hence the strong particle size dependence. The surface-particle contact area can be estimated by calculating how much the particle is pushed into the soft material due to the applied load by means of Hertzian theories. It should be noted that Hertzian theories consider two smooth surfaces in contact and do not consider the effect of neighboring particles. However, as we will demonstrate in the following sections, our results do appear to scale with the parameters estimated using the Hertzian-type analysis. This indicates that, although the absolute contact area values may vary, using the estimated values allows us to satisfactorily relate the frictional behavior to the contact mechanics.

Using Hertzian theories, we estimate the displacement d, which shows how much each particle is inserted into the PDMS surface and the contact area diameter a as $F_N = \frac{4}{3}E^*R^{1/2}d^{3/2}$ [30].

Here, F_N is the load per particle (0.5 N distributed over all particles on 2 mm^2), and E^* is the effective Young's modulus

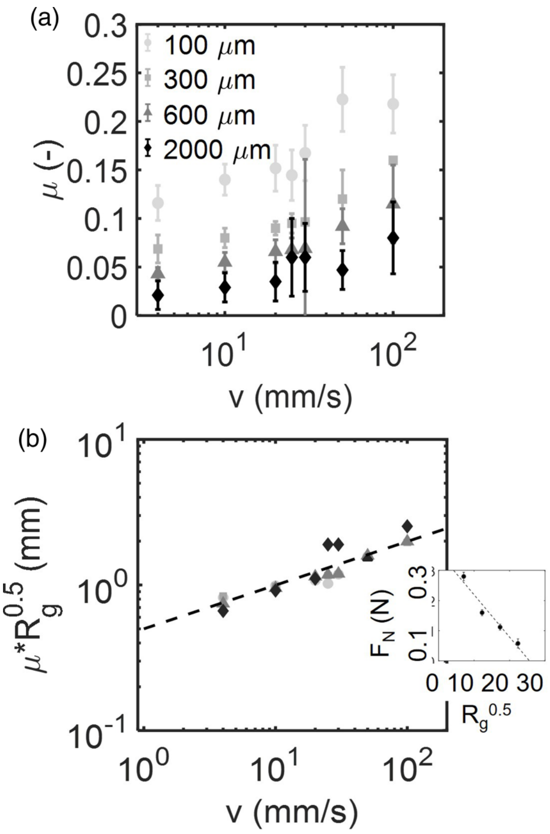

FIG. 2. (a) The friction coefficient as a function of maximum velocity for a range of lubricating particle diameter at 0.5 N measured with a rough (asperity width 100–400 μm) polydimethylsiloxane (PDMS) probe (diagram not to scale). (b) The collapsed data obtained when μ is multiplied by $R_g^{0.5}$. The scaling of $R_g^{0.5}$ with F_F is shown in the inset. The dashed lines represent an empirical fit through the data.

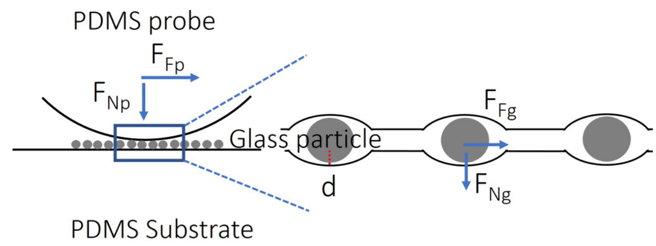

FIG. 3. Schematic view of the normal and friction forces acting on the probe (F_{Np}, F_{Fp}) and on the particles (F_{Ng}, F_{Fg}) and the indentation depth d.

of the PDMS (2.5 MPa). We use 2 mm^2 here because this is well above the estimated Hertzian contact area between the 2000 μm glass particle and the PDMS surface at 0.5 N ($\approx$1 mm). At 2 mm^2, we can thus assume that at least one 2000 μm particle will be present between the PDMS surfaces. For the particles of sizes 2000, 600, 300, and 100 μm, we find indentation depths of 282, 85, 42, and 14 μm, respectively. We therefore suggest that our observation of a friction coefficient increasing with decreasing particle size may be due to the corresponding increase in particle-substrate contact area. The theoretical contact area diameter a of a glass particle indenting the PDMS surface is defined as $a = (R_g d)^{0.5}$, with R_g the radius of the glass particle. We find values of 481, 145, 72, and 24 μm for the 2000, 600, 300, and 100 μm sized particles, respectively. The friction coefficient thus appears to decrease with increasing contact area.

The speed curves for the different particle sizes all appear to follow a similar increasing trend. When we multiply μ by $R_g^{0.5}$, we find that the data collapse onto a single line, shown here with a (dashed) trend line [Fig. 2(b)]. To understand the origin of this dependence of μ on $R_g^{0.5}$, we assess the friction and normal forces acting on the probe and a single particle (Fig. 3) using the Hertzian approach. For this, we use the normal force the PDMS probe (F_{Np}) exerts on each particle: $F_{Np} = (a/R^2)F_{Ng}$. We determine the normal force per glass particle as $F_{Ng} = E^* R_g^{0.5} d^{3/2}$. Using these two equations, we obtain $F_{Np} = aE^*(d/R_p)^{3/2}$. A similar approach as used here for the normal force can be used for the friction force, resulting in $F_{Fp} = (a/R^2)F_{Fg}$. Assuming that $F_F \propto$ the contact area, we then find that $F_{Fg} \propto R_g d$, and thus, $F_{Fp} \propto a(d/R_g)$. Since $\mu = F_F/F_N$, we then find that $\mu = F_{Fp}/F_{Np} \propto E^*(d/R_g^{0.5})$. This would mean that $\mu R_g^{0.5}$ should be constant at given speed and normal force. This scaling with R_g is verified in Fig. 2(b).

When we increase the sliding speed, we see an increase in the friction coefficient for all particle sizes [Fig. 2(a)]. At high speeds, particles may easily be pushed out of the contact, which could potentially lead to PDMS-PDMS contact. As the escaping of particles from between the surfaces occurs at random, the relatively large error bars observed here are to be expected.

For the rough surfaces used here, we expect smaller particles can enter the space between the asperities. When particles become trapped between asperities, their ability to roll could be inhibited, and friction coefficients are expected to increase. This was also found in a previous study, where the friction coefficient of rough PDMS surfaces lubricated by solid particles increased when particles were of similar size as the surface asperities [7]. When we compare friction coefficients of rough surfaces lubricated by 100 μm particles with smooth surfaces lubricated by the same particles, we find friction coefficients that are twice as large for the rough surfaces at high normal forces, as will be discussed in the next section. This shows that an increase in surface-surface and particle-surface contact area causes an increase in the friction coefficient. We will discuss this further in the following section.

Although particles enter the space between asperities, we do find that the friction coefficients of particle lubricated contacts are still far lower than the friction coefficient of a dry PDMS-PDMS contact. This is an indication that the particles can still prevent complete PDMS-PDMS contact.

B. Normal force dependence

We expect particle inclusion between the asperities to be enhanced at higher normal forces, due to the deformable nature of the surfaces. As the load increases, the elastic substrates can cover and entrain the lubricating particles due to deformation of the PDMS around the particles, causing increased direct PDMS-PDMS contact. From measurements at normal forces ranging from 0.25 to 1.5 N using both a

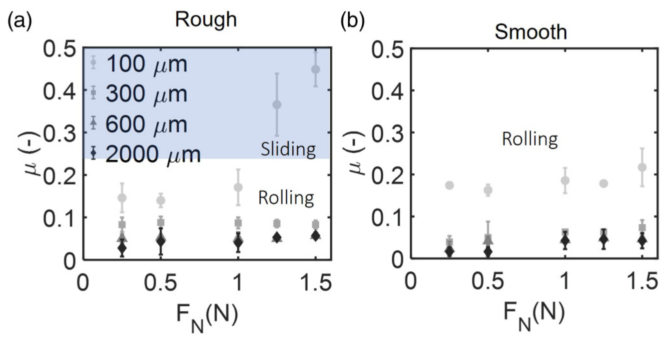

FIG. 4. Normal force F_N dependent friction for all particle sizes using (a) a rough and (b) a smooth probe. The transition from rolling to sliding friction is highlighted in blue.

rough probe and a smooth probe, we indeed find that higher normal forces give higher friction coefficients for the smallest (100 μm) particles [Figs. 4(a) and 4(b)]. The increase in friction coefficient as a function of the normal force is modest for larger particles, suggesting only a small contribution to the total dissipation from the few normal-force strengthened surface-particle contacts.

For the 100 μm particles, we find a threefold increase in friction coefficient from $\mu = 0.15$ to 0.45 when the normal force is increased from 0.25 to 1.5 N using the rough surface. While the contact area is expected to increase gradually with increasing normal forces, there appears to be a threshold F_N above which the friction coefficient increases strongly. This threshold force is most likely related to particles becoming entrained between the asperities of the rough PDMS (asperity size $\approx$ 100–400 μm) and the deformability of PDMS, which leads to a sudden change in contact dynamics with changes in F_N.

When the normal force increases, the indentation of the PDMS surfaces by the particles facilitates particle inclusion between the asperities and generates larger contact areas between the two surfaces and between the surfaces and the particles.

C. Rolling and sliding friction

An increase in normal force from 0.25 to 1.5 N for a glass particle on a PDMS plane gives an increase in contact area from 115 to 380 μm^2. This is related to an increase in indentation depth from 7 to 24 μm. For the rough surfaces, the actual contact area is higher as particles enter the space between the asperities, and therefore, more direct PDMS-PDMS contact will occur. In Fig. 4(b), it can be seen that the normal force dependence for smooth surfaces is much less pronounced compared with surfaces with asperities. For surfaces under higher load, we find two separate mechanisms that may affect the friction coefficient: (I) reduction in rolling capacity of particles due to inclusion between asperities causing particles to slide over the surface with increased glass-PDMS contact area and (II) direct PDMS-PDMS sliding contact.

The transition from rolling to sliding friction is visible in Fig. 4(a), where the contact regime (sliding friction) is highlighted in blue. This shows the contact area dependence of the friction coefficient. The smallest particles paired with the rough surface are most sensitive to changes in normal force as the particle-surface contact area increases rapidly for these surfaces where the asperities are of similar dimensions as the particles.

We visualize the particles entering the space between the asperities by means of optical microscopy. To observe how particles may be inserted between PDMS asperities, we placed particles between a (rough or smooth) PDMS probe and a flat glass microscope slide. The particles were then pushed against the PDMS surface at 0.5 and 1.5 N. In Fig. 5(a), in the top row, we observe PDMS-particle contact at 0.5 N compared with 1.5 N for the smooth probe. The difference in contact for the two forces is not very obvious, which is consistent with the similarity of the friction coefficients. Note that, to obtain informative images, a lower surface coverage of particles was used during imaging than in the tribology experiments. For the rough probe, we see that particles are inserted between the asperities at both low and high normal force. Additionally, we observe an increase in contact area at higher normal forces. Applying a black-and-white image filter makes it even more evident that more contact (white) is obtained at higher normal forces as particles (black) are pushed further into the PDMS surface [Fig. 5(b)]. These results show the major role that particle inclusion between the asperities and contact area play in the frictional behavior of deformable surfaces.

D. Partially covered surfaces

We previously suggested that the friction coefficient increases with increasing PDMS contact, for example, due to increased normal forces or enhanced particle insertion between asperities. To verify how the friction coefficient responds to increasing PDMS-PDMS contact, we designed an experiment where we varied the number of glass particles present on the surface. We eliminated the effect of particle trapping by using a smooth PDMS probe against a smooth PDMS surface and limited sliding speed to 10 mm/s and the normal force to 0.5 N. To maximize changes in surface-surface contact, we used the smallest particles which initially already gave a small gap size of maximum 100 μm, i.e., the diameter of the particles. We quantified surface coverage via the total area of particles covering the flat PDMS surface; we used the particle diameter to calculate its effective surface coverage and present surface coverage as a percentage of the total surface coverage (Fig. 6). Here, 100% refers to the substrate being completely covered with a randomly packed monolayer of particles. At low surface coverage, the friction coefficient is rather high ($\mu \approx 2$) and approaches the friction coefficient of dry PDMS ($\mu \approx 3$). As there are only a few particles present to separate the surfaces, direct PDMS-PDMS sliding contact is likely the cause for these high frictional values due to surface deformation or indentation. We find a steep decrease in friction coefficient as the percentage of particles increases. Higher particle surface coverage corresponds to less deformation, i.e., larger gap sizes, and less PDMS-PDMS contact, which leads to a decrease in friction as also seen in previous sections (Fig. 4). At a surface coverage of 1, 2, 5, and 10% and a normal force of 0.5 N, the estimated indentation depth using Hertzian theories equals 12, 18, 157, and 250 μm. As the latter values of indentation are larger than the particle

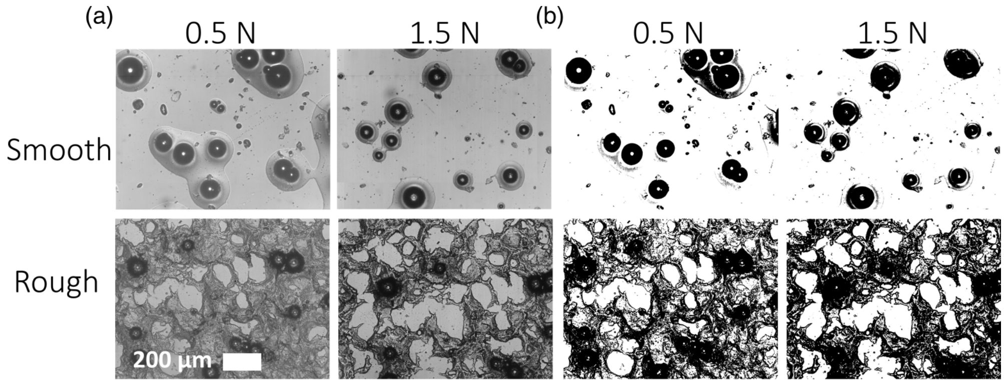

FIG. 5. (a) Microscopy images of smooth and rough polydimethylsiloxane (PDMS) surfaces in contact (white areas) with particles (dark areas) at 0.5 and 1.5 N for smooth (upper row) and rough (lower row) surfaces. In (b), the same images are shown with a black-and-white filter applied to emphasize PDMS contact and particle contact. Larger white areas are seen at high F_N, indicating larger contact areas and particle insertion between asperities. Low surface coverage was used here for imaging purposes. Scale bar represents 200 μm.

size (100 μm), the particles become fully enveloped by the PDMS surfaces, and direct PDMS contact arises.

The glass particles between PDMS surfaces already show optimal lubrication at only 10% surface coverage. For surface coverage values higher than 10% of particles, we see a constant friction coefficient. We can thus expect that 10% of particles distributes the total normal force over enough particles that the PDMS substrates do not deform enough to completely envelope the particles. Thus, PDMS-PDMS contact is limited, and the particles can roll between the PDMS surfaces. This regime of constant friction coefficient represents the rolling friction regime; values for μ here are indeed consistent with those shown in Fig. 4.

The surface coverage dependence measurements of hard-particle-lubricated soft substrates are an additional confirmation that there is a strong indentation depth or contact area dependence. Contact area dependencies are not uncommon for either soft or hard materials and have been shown to occur in different systems, such as elastic contacts [31] and, more specifically, hydrogels [17,18,32].

E. Varying the tribometer motion

To assess the robustness of the observations under different tribological circumstances, we varied the relative sliding and rolling motion of the sliding surfaces. To do this, we introduced an additional friction tester, the MTM, Fig. 7(a), which is known as a double drive tribometer. This tribometer can give us extra insights into the sliding-rolling effects, as the MTM can control the rotating PDMS ball and the sliding

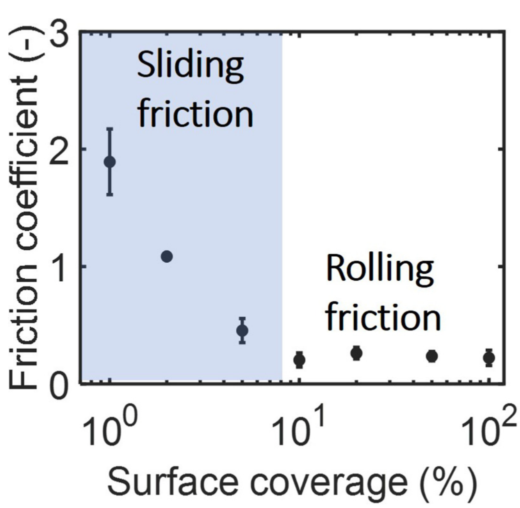

FIG. 6. Friction coefficient as a function of surface coverage for the 100 μm particles between a smooth hemispherical polydimethylsiloxane (PDMS) probe and a smooth flat PDMS substrate. Surface coverage is defined with respect to the maximum number of particles that geometrically fit in a single layer; see text.

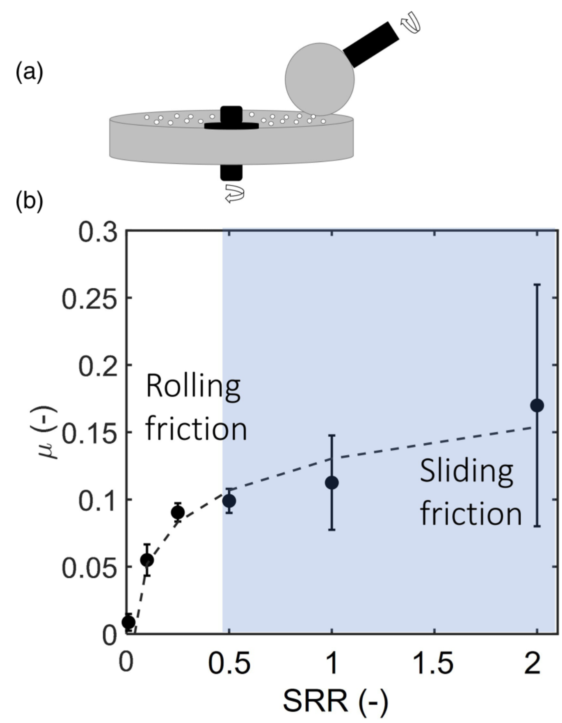

FIG. 7. (a) Schematic view of the Mini Traction Machine with two polydimethylsiloxane (PDMS) surfaces and glass particles as a lubricant. (b) Friction coefficient obtained using a double drive tribometer at various slide-to-roll ratios.

PDMS disk independently [20,26,28]. The MTM also allows us to answer an additional question: how does the surface motion (e.g., rolling or sliding probe and substrate) influence the contact area dependent friction coefficient? We use the 100 μm particles entrained between two smooth PDMS surfaces at 10 mm/s, as used previously, at a surface coverage of 100%. In this case, a normal force of 1 N is used to stay within the measuring range of the tribometer, and the probe is very similar to the probe used on the Bruker tribometer [diameter (hemi-)sphere on MTM tribometer: 19 mm, Bruker tribometer: 20 mm]. With the ability to drive the probe and substrate separately, we have the possibility to vary the ratio between the speed of the ball and the speed of the disk, also known as the SRR.

At SRR = 2, where pure sliding of the surfaces takes place, the frictional values are within the same range as observed previously for the same particles of 100 μm in diameter [$\mu_{\max} \approx 0.17$, Fig. 7(b)]. The expected transition from sliding to rolling friction is also seen using the MTM. We find a strong decrease in friction coefficient from 0.2 to ~0.008 when we decrease the SRR from 2 to 0. When the ball and disk are rotating at equivalent velocities, i.e., SRR = 0, the spherical particles are easily maintained between the surfaces and are allowed to roll along with the imposed motion of the PDMS surfaces. The rolling of the particles is then driven by both the ball and the disk, which results in extremely low friction coefficients. At higher SRRs, the rolling of the particles is mainly driven by only one of the surfaces at a time, while the stationary surface counteracts the rolling motion of the particles. Additionally, at high SRR values, particles can be expected to leave the contact regime and accumulate around the probe, which would result in high friction as well. Once particles exit the gap, large PDMS contact areas lead to increased friction coefficient. Particles exit the gap at different times and speeds during each measurement, which explains the large error bars observable in Fig. 7(b). The increase in friction with decreased particle rolling ability shows that restricted particle rolling motion causes an increase in friction coefficient, which was also seen when varying measuring parameters including the normal force in previous sections.

F. Relating the friction coefficient to the contact area

We have highlighted the transition from rolling (particle) friction to sliding (surface dominated) friction by varying the particle size, normal force, surface roughness, number of particles, and even by using an additional tribological device. As the friction coefficient is often related to the contact area, we combine the friction coefficients from the measurements in previous sections performed with the smooth probe into one figure, as a function of the contact area radius estimated using a Hertzian approach (Fig. 8).

Using this approach, we show that the friction coefficient in the rolling regime scales with $R_a^{-0.5}$, with R_a the radius of the contact area. The friction coefficient thus decreases with increasing contact area for the particles with different particle sizes. When the contact area increases due to increases in normal force or decrease in surface coverage, the friction coefficient increases. In the latter case, particle insertion and PDMS-PDMS contact causes the increase in friction

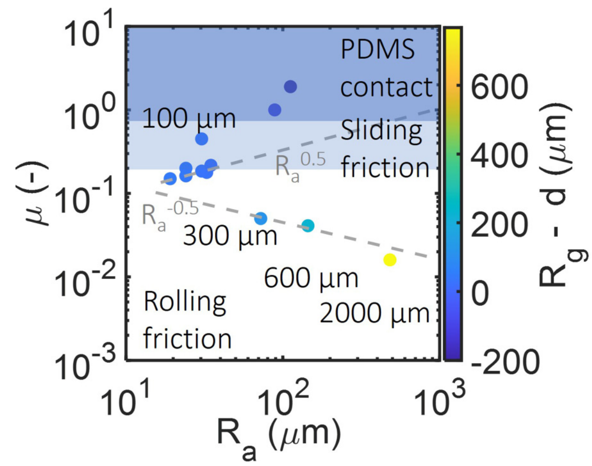

FIG. 8. Frictional values of Figs. 2, 4, 6, and 7 are combined to display the friction coefficient as function of contact area radius (R_a). The color bar represents $R_g - d$, which results in rolling, sliding or PDMS-PDMS contact friction.

coefficient. We attempt to quantify the increase of particle-particle and surface-particle contact and calculate the separation distance between the two PDMS surfaces by subtracting the indentation depth from the particle size; when the indentation depth is larger than the particle size, the PDMS surfaces are allowed to contact one another. We must note that PDMS is a viscoelastic material, and surface deformation can lead to internal dissipation at the surface or within the bulk of the material. However, these effects often become significant at either low sliding speeds or at higher deformation rates [33,34], and therefore, we consider these negligible. This scaling with the Hertzian contact mechanics parameters shows that the change in the contact area (rather than effects caused by internal dissipation) is the main contributor to the frictional behavior observed here.

From the color bar in Fig. 8 showing $R_g - d$, we see that an increase in this value causes a decrease in the friction coefficient for the particles of different sizes. For the 100 μm particles, we find that, when particles are pushed into the soft surfaces and are still able to keep the surfaces separated ($R_g - d \approx 40$ μm), relatively low friction coefficients are obtained. Once PDMS-PDMS contact is established ($R_g - d < 0$ μm), a strong increase in the friction coefficient is seen in this PDMS contact regime. This shows that each frictional regime has its own complex relation with the contact area depending on the particle-surface and surface-surface dynamics.

The lowest friction coefficients are seen for the larger particles that are well able to keep the surface apart (large $R_g - d$ values) in the rolling friction regime. When the separation distance falls below 100 μm, the particles are less able to separate the surfaces. Below this gap size, particle insertion into the PDMS surface begins to take place due to elastomeric surface deformation, and PDMS-PDMS contact is enlarged. We therefore propose the following mechanism: As particles have limited rolling ability, friction is dominated by sliding surfaces. This change from rolling particles to particles being pushed into and deforming the surfaces marks the onset of the sliding regime, as indicated in Fig. 8 in blue. Sliding here refers to the limited rolling ability of the particles due to insertion into the surfaces and enhanced particle-PDMS contact. The separation distance between the surfaces decreases further as the normal force increases or when there are less particles present on the surface. Both conditions lead to a higher normal force per particle, i.e., more surface deformation and higher surface-particle contact area and, with that, higher friction coefficients. When the glass-PDMS indentation depth is larger than the particle size, negative values are found for the indentation depth. We find indentation depths larger than the particle size at a surface coverage of 2 and 1%. At these percentages of surface coverage, particles are fully enveloped by the surfaces, and direct PDMS-PDMS sliding contact occurs.

This supports our suggested frictional mechanism: For large separations, low (or even no) direct PDMS-PDMS contact is expected, and low friction coefficients are found. As the separation distance decreases due to a decrease in particle size, particle number, or an increase in normal force, the overall indentation increases, and the friction coefficient increases accordingly. Once the surfaces are in contact, a large increase in friction is measured. We thus show that the degree of separation between the PDMS surfaces, as caused by changes in normal force and particle size of surface coverage, determines in what contact regime the frictional system is located. Based on the contact regime (PDMS contact, sliding, or rolling), the friction coefficient shows a positive or negative dependence on the contact area of the contact between the glass particles and the PDMS surface.

IV. CONCLUSIONS

In this paper, we used two tribometers to assess the frictional dynamics of dry hard spherical particles lubricating soft surfaces. We find that the friction coefficient increases with increasing normal force, when we decrease the number of particles on the surface and when smaller particles are used. The increase in friction coefficient in these cases is attributed to more surface-surface and particle-surface contact.

By manipulating different aspects of this soft-hard tribosystem, we display three different frictional regimes: a rolling regime, a sliding regime, and a PDMS-PDMS contact regime. The rolling regime displays low friction coefficients, attributed to the rolling motion of the particles. In the sliding regime, an increase in friction coefficient is found as particles are inserted between asperities due to similarity in size between particles and asperities. In this regime, particle-surface and surface-surface interactions arise, leading to an increase in friction coefficients. When the particles are fully covered by the surfaces (particle insertion and PDMS deformation), direct PDMS-PDMS contact takes place, and the friction coefficient increases accordingly.

ACKNOWLEDGMENTS

We would like to thank Heather Shewan for fruitful discussions. We wish to acknowledge funding by the Graduate School VLAG, travel funding from LEB fund Wageningen, and the Australian Research Council Discovery Project DP180101919 on Multiscale Viscoelastic Lubrication of Soft Matter Systems.

[1] O. Reynolds, IV. On the theory of lubrication and its application to Mr. Beauchamp tower's experiments, including an experimental determination of the viscosity of olive oil, Philos. Trans. R. Soc. London **177**, 157 (1886).

[2] P. M. Lugt and G. E. Morales-Espejel, A review of elasto-hydrodynamic lubrication theory, Tribol. Trans. **54**, 470 (2011).

[3] R. Stribeck, *Kugellager für beliebige Belastungen* (Buchdruckerei AW Schade, Berlin, 1901).

[4] D. Dowson, *History of Tribology* (Addison-Wesley Longman Limited, Boston, MA, 1979).

[5] R. N. Katz and J. G. Hannoosh, Ceramics for high performance rolling element bearings: A review and assessment, Int. J. High Technol. Ceram. **1**, 69 (1985).

[6] A. Singh, P. Chauhan, and T. Mamatha, A review on tribological performance of lubricants with nanoparticles additives, Mater. Today Proc. **25**, 586 (2019).

[7] F. Deng, G. Tsekenis, and S. M. Rubinstein, Simple Law for Third-Body Friction, Phys. Rev. Lett. **122**, 135503 (2019).

[8] B. K. Fussell, Analysis and performance comparison of a tooth wound brushless CPU cooling fan motor, in *Proceedings: Electrical Insulation Conference and Electrical Manufacturing and Coil Winding Technology Conference (Cat. No. 03CH37480)* (IEEE, New Jersey, 2003), pp. 379–386.

[9] F. Ebert, Performance of silicon nitride (Si_3N_4) components in aerospace bearing applications, in *Proceedings of the ASME 1990 International Gas Turbine and Aeroengine Congress and Exposition. Volume 5: Manufacturing Materials and Metallurgy; Ceramics; Structures and Dynamics; Controls, Diagnostics and Instrumentation; General, Brussels, Belgium, June 11–14, 1990* (ASME, New York, 1990).

[10] C. H. E. N. Guo, Nonlinear dynamic response analysis of unbalance-rubbing coupling faults of rotor-ball bearing-stator coupling system, J. Aerospace Power **22**, 1771 (2007).

[11] L. Peña-Parás, H. Gao, D. Maldonado-Cortés, A. Vellore, P. García-Pineda, O. E. Montemayor, K. L. Nava, and A. Martini, Effects of substrate surface roughness and nano/micro particle additive size on friction and wear in lubricated sliding, Tribol. Int. **119**, 88 (2018).

[12] S.-T. Kim, J.-Y. Woo, and Y.-Z. Lee, Friction, wear, and scuffing characteristics of marine engine lubricants with nanodiamond particles, Tribol. Trans. **59**, 1098 (2016).

[13] R. Aghababaei, Effect of adhesion on material removal during adhesive wear, Phys. Rev. Materials **3**, 063604 (2019).

[14] B. N. Persson, Theory of rubber friction and contact mechanics, J. Chem. Phys. **115**, 3840 (2001).

[15] B. N. Persson, U. Tartaglino, O. Albohr, and E. Tosatti, Rubber friction on wet and dry road surfaces: The sealing effect, Phys. Rev. B **71**, 035428 (2005).

[16] A. Schallamach, The load dependence of rubber friction, Proc. Phys. Soc., B **65**, 657 (1952).

[17] J. P. Gong, Friction and lubrication of hydrogels-its richness and complexity, Soft Matter **2**, 544 (2006).

[18] R. E. Rudge, E. Scholten, and J. A. Dijksman, Natural and induced surface roughness determine frictional regimes in hydrogel pairs, Tribol. Int. **141**, 105903 (2020).

[19] J. M. Urueña, A. A. Pitenis, R. M. Nixon, K. D. Schulze, T. E. Angelini, and W. G. Sawyer, Mesh size control of polymer fluctuation lubrication in gemini hydrogels, Biotribology **1**, 24 (2015).

[20] J. Bongaerts, K. Fourtouni, and J. Stokes, Soft-tribology: lubrication in a compliant pdms–pdms contact, Tribol. Int. **40**, 1531 (2007).

[21] N. Selway, V. Chan, and J. R. Stokes, Influence of fluid viscosity and wetting on multiscale viscoelastic lubrication in soft tribological contacts, Soft Matter **13**, 1702 (2017).

[22] J. Yu, S. Chary, S. Das, J. Tamelier, K. L. Turner, and J. N. Israelachvili, Friction and adhesion of gecko-inspired PDMS flaps on rough surfaces, Langmuir **28**, 11527 (2012).

[23] R. E. Rudge, J. P. van de Sande, J. A. Dijksman, and E. Scholten, Uncovering friction dynamics using hydrogel particles as soft ball bearings, Soft Matter **16**, 3821 (2020).

[24] A. Sarkar, F. Kanti, A. Gulotta, B. S. Murray, and S. Zhang, Aqueous lubrication, structure and rheological properties of whey protein microgel particles, Langmuir **33**, 14699 (2017).

[25] G. Yakubov, T. Branfield, J. Bongaerts, and J. Stokes, Tribology of particle suspensions in rolling-sliding soft contacts, Biotribology **3**, 1 (2015).

[26] C. Myant, H. Spikes, and J. Stokes, Influence of load and elastic properties on the rolling and sliding friction of lubricated compliant contacts, Tribol. Int. **43**, 55 (2010).

[27] J. De Vicente, J. Stokes, and H. Spikes, The frictional properties of newtonian fluids in rolling-sliding soft-EHL contact, Tribol. Lett. **20**, 273 (2005).

[28] J. De Vicente, J. Stokes, and H. Spikes, Rolling and sliding friction in compliant, lubricated contact, Proc. Inst. Mech. Eng. J **220**, 55 (2006).

[29] I. Penskiy, A. Gerratt, and S. Bergbreiter, Friction, adhesion and wear properties of pdms films on silicon sidewalls, J. Micromech. Microeng. **21**, 105013 (2011).

[30] K. L. Johnson and K. L. Johnson, *Contact Mechanics* (Cambridge University Press, Cambridge, 1987).

[31] B. Weber, T. Suhina, T. Junge, L. Pastewka, A. Brouwer, and D. Bonn, Molecular probes reveal deviations from Amontons' law in multi-asperity frictional contacts, Nat. Commun. **9**, 888 (2018).

[32] J. M. Urueña, E. O. McGhee, T. E. Angelini, D. Dowson, W. G. Sawyer, and A. A. Pitenis, Normal load scaling of friction in gemini hydrogels, Biotribology **13**, 30 (2018).

[33] P. F. Ibáñez-Ibáñez, F. J. M. Ruiz-Cabello, M. A. Cabrerizo-Vílchez, and M. A. Rodríguez-Valverde, Contact line relaxation of sessile drops on PDMS surfaces: A methodological perspective, J. Colloid Interface Sci. **589**, 166 (2021).

[34] J. H. Snoeijer, E. Rolley, and B. Andreotti, Paradox of Contact Angle Selection on Stretched Soft Solids, Phys. Rev. Lett. **121**, 068003 (2018).